



Modified arithmetic Mean Filtering algorithm for Optimal Generation of InSAR-derived Mosaics of Permafrost Active Layer Thickness

Dr.R.Rajeswari¹, Dr.G.Nirmalapriya²

Professor, Department of ECE, *Rajalakshmi Institute of Technology, Chennai, India*¹

Professor, Department of ECE, *Rajalakshmi Institute of Technology, Chennai, India*²

Abstract: Large-scale thawing of arctic permafrost results in the release of CO₂ and methane. This leads in global warming. Active Layer Thickness (ALT) is the maximum depth of thaw on the soil surface. The World Meteorological Organization (WMO) accepts it as an essential climate variable for monitoring the status of permafrost. Interferometric Synthetic Aperture Radar (InSAR) is a widely-used geophysical technique for measuring surface deformation at high spatial resolution. In recent years, InSAR has been successfully used to measure ground deformation due to seasonal permafrost thaw cycles and invert this deformation signature for a spatially extensive and finely-sampled map of ALT. This paper presents a novel method to estimate active layer thickness (ALT) over permafrost based on InSAR (Interferometric Synthetic Aperture Radar) observation.

Keywords: permafrost, permafrost dynamics, active layer thickness, interferometric synthetic aperture radar

I. INTRODUCTION

The aim of this project is to extend various image processing techniques towards an area of active research in the geophysical climate community. Interferometric synthetic aperture radar (InSAR) is a well-established radar remote sensing technique (Rosen et al. 2000). The synthetic aperture radar (SAR) technique utilizes the principle of coherent radar pulse integration, and doppler processing to generate high resolution (~5-10 m pixel resolution) radar images of the earth's surface from earth-orbiting satellites (Rosen et al. 2000). Each pixel in a SAR image is a complex variable with amplitude associated with the amount of returned scattered energy from the earth's surface that is received by the radar, and a phase associated with the total distance from the radar unit to the earth's surface. When multiple SAR images over a single region of interest are acquired, the (element-wise) product of one image with the complex conjugate of the other image yields the difference in phase between these two images. Because this phase is directly related to distance, this image of phase difference (referred as interferogram), encapsulates information related to the earth's topography, and any surface deformation that occurred in-between the acquisition times of the two images (citation needed). If a priori information of the earth's topography is available (conventionally a digital elevation

model, or DEM), the topographic phase dependency can be removed from an interferogram, leaving behind the surface deformation signature and noise. InSAR has a well-established heritage in studying the surface deformation associated with earthquakes, volcanoes, glacial ice flow, landslides, and ground subsidence (citation needed) [1]. In recent years, the InSAR technique has been used to study the ground deformation associated with freeze/thaw surface subsidence in arctic permafrost environments. Permafrost environments are regions that are cold enough such that the groundwater held in the pore space of soils is completely frozen for a significant portion of the year. During the spring thaw period, rising surface temperatures cause pore space water to gradually thaw from solid to liquid; because a given amount of water takes more volume in its solid state than its liquid state, this phase change of water causes the ground to subside (or 'sink' downwards) due to the effective decrease in volume in a column of soil during thaw. As the spring season progresses through summer, extended periods of above-zero surface temperature cause more and more of the subsurface pore water to thaw, thereby causing a greater amount of subsidence. Eventually, a given region of permafrost will experience its maximum thaw during the thaw season; the depth to which the subsurface has thawed is referred to as the active layer thickness (ALT). In autumn and winter, this liquid water freezes again, and the ground



experiences uplift (or 'rises' upward) as the effective volume of the pore space in a soil column increases [5]. Thus, over a seasonal cycle, permafrost environments experience freeze/thaw-associated cycles of ground deformation, which can be imaged and characterized by InSAR. [2] Permafrost regions contain large amounts of CO₂ and methane within the shallow subsurface and repeat thaw of permafrost can cause these greenhouse gases to be released into the atmosphere. Permafrost regions are thus a significant source of greenhouse gas emissions, and the process by which these gases are emitted is often a positive (unstable) feedback loop. Fully understanding the dynamics of permafrost freeze/ thaw cycles is of high importance within the climate scientific community, and currently this process is not completely understood. InSAR therefore is a promising technique that helps in understanding the earth system process. The ReSALT (Remotely-Sensed Active Layer Thickness) technique, utilizes InSAR-derived surface deformation to invert for ALT across SAR scenes [6]. This technique generates broad, regional distributions of ALT at a spatial scale of 10 meters a significant improvement on existing methods of regional ALT characterization.

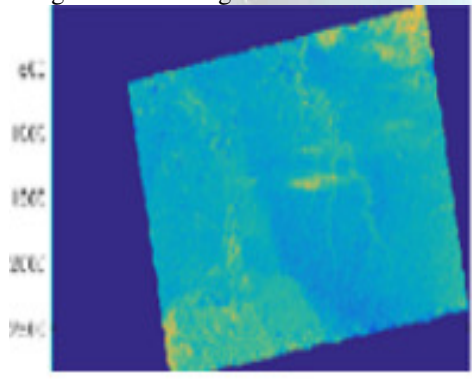


Fig 1: unmasked Interferogram

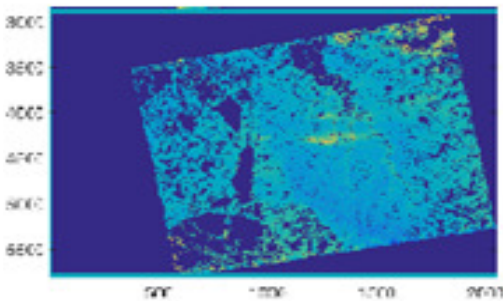


Fig 2: Interferogram Masked with the phase-variance thresholding mask.



Fig 3: Comparison of the mask's derived edges with surface optical imagery. The phase variance thresholding mask successfully masks out water regions, and preserves borders.

II. METHODOLOGY

Two image processing techniques that are directly applicable towards the ReSALT method have been developed to help in getting the 1) Large range of permafrost environments, and 2) Generate larger regional distribution maps of ALT[3]. For this a phase-variance-based threshold masking routine, which successfully delineates surface features that are consistently wet (lakes, rivers, thaw ponds, etc) is developed. These features bias the ReSALT technique with false, nonphysical estimates of active layer thickness (ultimately due to the scattering interaction between radar pulses and water surfaces), and thus must be masked out of ALT maps. The phase variance masking routines takes advantage of the scattering interaction of radar pulses with water surfaces to directly identify regions within an interferogram that are water surfaces (without the use of secondary information such as optical imagery), and then mask out these regions. Secondly, a modified weighted arithmetic mean mosaicking algorithm that can be used to stitch together several scenes of estimated ALT is proposed. Thus the larger regions of ALT can be characterized. Instead of using a conventional mosaicking technique, a method that took into account the uncertainties in measured ALT as a weighting method is proposed. Ideally the mosaicking algorithm do not bias the measured values of ALT.[5]

III. PHASE VARIANCE MASK

The phase variance of each interferogram is calculated. This algorithm calculates the phase variance (1) associated with each pixel in an interferogram, and for each pixel, returns

$$1 - \left(\frac{\text{variance}}{\text{threshold_variance}} \right) \quad (1)$$

where threshold variance is an input value for the expected maximal variance in a scene. For each SAR stack of N coregistered interferograms, the sum of the output of this phase variance (2) algorithm is considered.

$$V_{ij} = \sum_{k=1}^N \max \left[0, \left(1 - \frac{\sigma_{ij,k}}{\sigma_{\text{threshold}}} \right) \right] \quad (2)$$

This output, $V(i,j)$ is therefore the sum total of phase variance per pixel in a stack of interferograms, rescaled such that a pixel value of 0 corresponds to a pixel whose variance is consistently greater than $\sigma_{\text{threshold}}$ in all N interferograms, and a pixel value of N corresponds to a pixel whose variance is 0 in all N interferograms. Then the different threshold values of $V(i,j)$ are examined to use as a phase-variance mask to mask out unwanted regions (lakes, rivers, swamps, marshes) whose estimates of ALT are nonphysical. It is found that a simple threshold of 0 successfully removes these regions, and sharply preserves the borders of these regions (up to the SAR resolution).

$$M_{ij} = 1 \text{ for } V_{ij} > 0 \quad (3)$$

$$M_{ij} = 0 \text{ for } V_{ij} = 0 \quad (4)$$

Unmasked ALT (top) and Masked ALT (bottom)

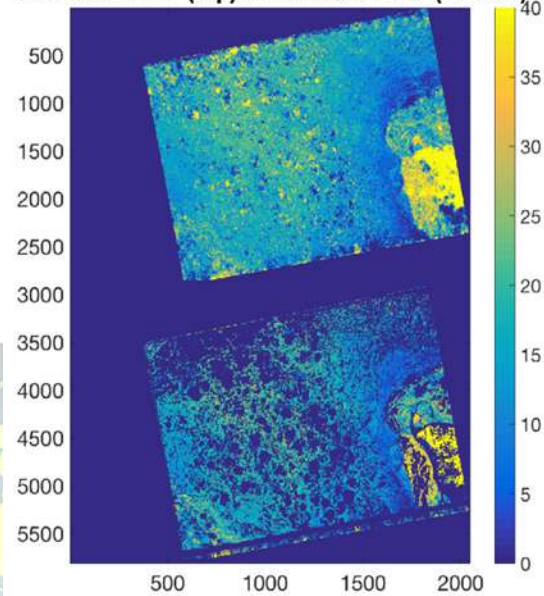


Fig 4: (Top) ALT distribution unmasked (top) and masked using the phase variance threshold mask (bottom). Notice that the mask successfully removes anomalous, unphysical large estimates of ALT that occur at the surface of thaw ponds (bright yellow at top, masked out at bottom).

IV. WEIGHTED ARITHMETIC MEAN MOSAICKING ALGORITHM

The algorithm used to invert deformation for ALT is similarly not included in my final report, as it is beyond the scope of this course. This algorithm inverts deformation for ALT using a functional relationship deformation and active layer thickness that depends upon soil porosity, saturation, organic matter content, and density contrasts and distributions within the soil column. The output of the algorithm is an estimate of ALT, and associated uncertainties from the model. These images are included within each SAR stack sub directory, and the associated latitude and longitude ranges of each geocoded stack.

The weighted arithmetic mean mosaicking algorithm developed utilizes the ALT and ALT uncertainty images for each stack, as well as their associated latitude and longitude ranges as inputs. The algorithm first determines the spatial offsets between each image, and generates a global scene within which it places each image. Then, the algorithm determines the regions of overlap between all of the images, and performs a weighted arithmetic mean of each overlapping image, using the ALT image's associated uncertainties as its weighting term. I.E:

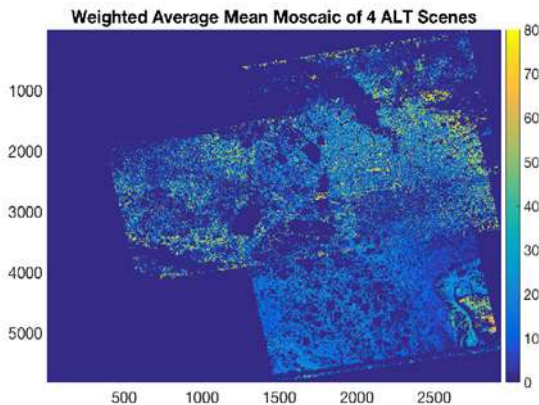


Fig 5: Georeferenced global mosaic of 4 separate images of ALT distribution. Images are coregistered using their respective geographic information from SAR processing, and are mosaicked together with the weighted arithmetic mean algorithm. This technique ‘blends’ along the discontinuous edges of each image, while keeping ALT estimates physically realistic by using the associated pixel uncertainty values as the weighting elements.

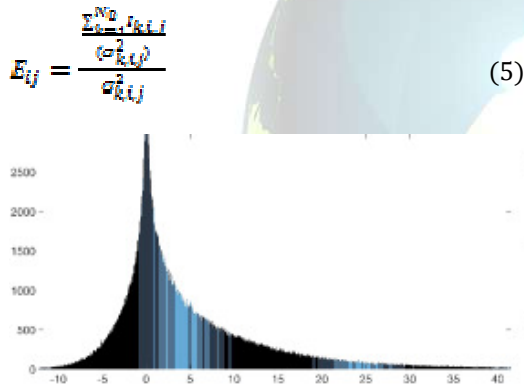


Fig 6: Histogram of values for the difference between the weighted arithmetic mean mosaic and simple averaging technique.

The output mosaic is compared to mosaics generated with a simple averaging technique. The weighted arithmetic mean is seen to produce ‘smoother’ distributions of ALT when compared to these simpler mosaicking routines. Furthermore, by incorporating actual uncertainty measurements into the estimate, this averaging routine does not introduce artificial biases into the physical ALT estimate in regions of image overlap. [4] proposed a method in which the minimization is performed in a sequential manner by the fusion move algorithm that uses the QPBO min-cut algorithm. Multi-shape GCs are proven to be more beneficial than single-shape GCs. Hence, the segmentation methods are validated by calculating statistical measures. The false

positive (FP) is reduced and sensitivity and specificity improved by multiple MTANN.

V MODIFIED WEIGHTED ARITHMETIC MEAN MOSAICKING ALGORITHM

The Modified weighted arithmetic mean mosaicking algorithm developed uses both the ALT and ALT uncertainty images of each stack, as well as their associated latitude and longitude ranges as inputs with the weighting element W_{ij} . Similar to the weighted arithmetic mean mosaicking algorithm it first determines the spatial offsets between each image, and generates a global scene within which it places each image. Then, the algorithm determines the regions of overlap between all of the images, and generates a modified weighted of each overlapping image, using the ALT image’s associated uncertainties as its weighting term.

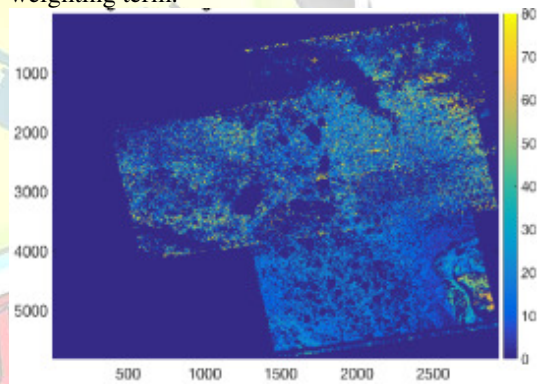


Fig 7: Georeferenced global mosaic of 4 separate images of ALT distribution. Images are co-registered using their respective geographic information from SAR processing, and are mosaicked together with the modified weighted arithmetic mean algorithm.

$$E_{ij} = W_{ij} \frac{\sum_{k=1}^{No} I_{k,i,j}}{\sum_{k=1}^{No} \sigma_{k,i,j}^2} \quad (6)$$

The output mosaic is compared to mosaics generated with a simple averaging technique. The modified weighted arithmetic mean produce ‘smoother’ distributions of ALT when compared to these simpler mosaicking routines. Furthermore, by incorporating actual uncertainty measurements into the estimate, this averaging routine does not introduce artificial biases into the physical ALT estimate in regions of image overlap.



The output of modified weighted arithmetic mean mosaic is compared to mosaics generated with a weighted arithmetic mean mosaic. The modified weighted arithmetic mean is seen to produce 'smoother' distributions of ALT when compared to these simpler mosaicking routines. Furthermore, by incorporating actual uncertainty measurements into the estimate, this averaging routine does not introduce artificial biases into the physical ALT estimate in regions of image overlap.

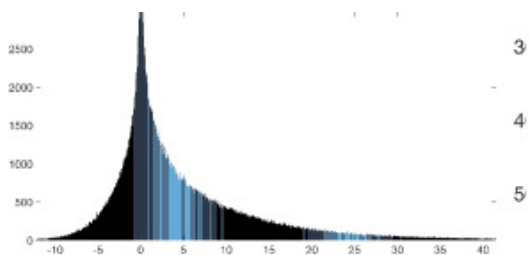


Fig 8: Histogram of values for the difference between the weighted arithmetic mean mosaic and Modified weighted arithmetic mean mosaic.

The figure.6 shows that Most of the values are centered at zero (pixels with no overlap between images), but significant deviations between the two methods occur for regions of image overlap.

VI. CONCLUSION

The phase-variance threshold masking technique successfully pixels associated with poorly-correlated surface water regions. By using phase variance as a threshold, this mask sharply preserves the edges of water features, and drastically improves scene-wide estimates of active layer thickness by removing false values associated with these water features. The weighted arithmetic mean mosaicking algorithm successfully co-geolocates several different InSAR stack scenes within a single global scene. Additionally, the algorithm 'blends' regions of image overlap by using a weighting averaging scheme that utilizes model uncertainty as a weight. This improves active layer thickness estimates by reducing uncertainties in regions of image overlap, and allows for the generation of large, regional distributions of active layer thickness. The modified weighted arithmetic mean still more successfully co-geolocates several different InSAR stack scenes within a single global scene as the weight factor is varied with the inclusion of the weight component W_{ij} . This component improves the demarcation of the land from the water and snow features. These techniques improved the ReSALT technique performance in wetland arctic regions, and can

help generate more complete distribution maps of active layer thickness for climate change studies.

REFERENCES

- [1] Rosen P. A. et al. 2000 , Synthetic Aperture Radar Interferometry', Proc. IEEE, vol. 88, no. 3.
- [2] R. M. Goldstein and C. L. Werner, "Radar interferogram filtering for geophysical applications," Geophys. Res. Lett., vol. 25, no. 21, pp. 4035–4038, 1998.
- [3] A. M. Guarnieri and C. Prati, "SAR interferometry—A quick and dirty coherence estimator for data browsing," IEEE Trans. Geosci. Remote Sensing, vol. 35, pp. 660–669, 1997
- [4] Christo Ananth, G.Gayathri, M.Majitha Barvin, N.Juki Parsana, M.Parvin Banu, "Image Segmentation by Multi-shape GC-OAAM", American Journal of Sustainable Cities and Society (AJSCS), Vol. 1, Issue 3, January 2014, pp 274-280.
- [5] Liu L. et al. 2014, Seasonal thaw settlement at drained thermokarst lake basins, Arctic Alaska. Cryosphere 8, 815–826 .
- [6] Barbara et.al. 2017, Active-layer thickness estimation from X-band SAR backscatter intensity, The Cryosphere, 11, 483–496